



Queensland University of Technology
Brisbane Australia

This is the author's version of a work that was submitted/accepted for publication in the following source:

Elunai, Ronald, Chandran, Vinod, & Mabukwa, Prosper (2010) Digital image processing techniques for pavement macro-texture analysis. In Doyle, Neil (Ed.) *Proceedings of the 24th ARRB Conference: Building on 50 years of road transport research*, ARRB Group Ltd., Sebel Hotel, Melbourne, Vic, pp. 1-5.

This file was downloaded from: <http://eprints.qut.edu.au/40770/>

© Copyright 2010 [please consult the Authors]

Notice: *Changes introduced as a result of publishing processes such as copy-editing and formatting may not be reflected in this document. For a definitive version of this work, please refer to the published source:*

DIGITAL IMAGE PROCESSING TECHNIQUES FOR PAVEMENT MACRO-TEXTURE ANALYSIS

Ronald Elunai^{1,2}, Vinod Chandran², Prosper Mabukwa¹

¹Transport and Main Roads, Queensland, Australia

²Queensland University of Technology, Queensland, Australia

ABSTRACT

Road surface macro-texture is an indicator used to determine the skid resistance levels in pavements. Existing methods of quantifying macro-texture include the sand patch test and the laser profilometer. These methods utilise the 3D information of the pavement surface to extract the average texture depth. Recently, interest in image processing techniques as a quantifier of macro-texture has arisen, mainly using the Fast Fourier Transform (FFT). This paper reviews the FFT method, and then proposes two new methods, one using the autocorrelation function and the other using wavelets. The methods are tested on pictures obtained from a pavement surface extending more than 2km's. About 200 images were acquired from the surface at approx. 10m intervals from a height 80cm above ground. The results obtained from image analysis methods using the FFT, the autocorrelation function and wavelets are compared with sensor measured texture depth (SMTD) data obtained from the same paved surface. The results indicate that coefficients of determination (R^2) exceeding 0.8 are obtained when up to 10% of outliers are removed.

INTRODUCTION

Road surface macro-texture is an important parameter of road design for highway engineers. It is a contributor to road noise and spray. In wet weather, macro-texture provides extra drainage capacity in addition to that provided by tyre treads, thus minimising skidding. Consequently, highway engineers seek to provide adequate macro-texture on roads, commensurate with the traffic speed to ensure that road safety requirements are met, while at the same time keeping the levels of noise and spray to tolerable levels. Such an optimisation approach to road surface macro-texture maintenance requires continual monitoring throughout the life of the road surface.

The earliest and most fundamental method for measuring road surface macro-texture is the volumetric sand patch test. Here a known volume of sand is spread on a road surface to form a nearly flat disc, in level with the road surface. The depth of the disc, which is the known volume of sand divided by the disc area, constitutes the surface texture depth. Road surface macro-texture as depth is commonly measured in mm.

It is obvious that the sand patch test is too slow to be conducted in busy traffic, and requires lane closure for the duration of the test. These were some of the reasons for developing the laser profiler method, which could measure texture depth even at highway speeds. The accuracy of the laser profiler method through its correlation with the sand patch test is demonstrated in (Choi 2008).

The circular texture meter (ASTM 2005) is another laser based method. It mimics the sand patch test, by measuring depth in a circular pattern rather than taking longitudinal scans as done by the laser profilometer. A comprehensive review of existing methods for macro-texture measurement can be found in (Choi 2008).

The idea of employing image processing techniques for road surface macro-texture dates back to 1970 (Schonfeld 1970). However, owing to the development and refinement of the laser profilometer technique as a substitute for sand patch tests, photographic methods underwent a period of hibernation until the start of this decade. The work by Gransberg *et al* (Gransberg 2002) involved the analysis of road surfaces using the Fast Fourier transform (FFT), where it was observed that deteriorating road surfaces display a lower maximum FFT magnitude value than roads in good condition.

In (Pidwerbesky *et al* 2006) the sand patch test method for pavement surface texture determination was correlated with FFT outputs from the images of the same surfaces. Coefficients of determination of up to 0.93 were registered. However, the data points used in the study were limited (less than 10 points), and one of the suggestions made by the authors was to conduct similar experiments with more data for reliability. A significant finding of the study was that road surface macro-texture responds optimally to certain frequency bands in the FFT domain. This relationship between macro-texture and frequency bands was further confirmed in (El Gendy and Shallaby 2008). These findings regarding band selectivity in macro-texture are in keeping with the classification of road surface characteristics coined in the 18th world congress report (PIARC 1987) in which macro-texture is placed in the range between 0.5mm and 50mm

In retrospect, the analysis of road surface texture using digital image processing combines two existing broad fields of study, namely, spectral/statistical texture analysis and optical granulometry. Spectral/Statistical texture analysis dates back to the seventies and early eighties. Tamura *et al* (Tamura 1978) developed computational textural features that would correspond to the human visual system and Laws (Laws 1980) developed textural features that are suited for machine analysis of textures. These were amongst the pioneering works that shaped the field of visual texture analysis using computer vision. Some of the main features examined were by Tamura and Law included coarseness, directionality and regularity. In this paper we shall focus is on the coarseness feature because of its closeness to the concept of texture depth.

Optical granulometry is the measurement of the distribution of size in a collection of grains using mathematical morphology or other image processing techniques. An example of granulometric approach is the application of morphological techniques to grain size distribution in gravel (Butler 2002).

In this paper we examine whether the statistical and spectral texture analysis methods and especially the coarseness feature in textures, can be adapted for the analysis of road surface, and particularly, texture depth. This paper is organised as follows: First we review the relationship between texture coarseness as defined in the texture analysis literature, and 3D texture depth. We then explore some of the common statistical/spectral texture coarseness characterisation techniques. We conclude by presenting and discussing a comparison of results between SMTD (Sensor Measured Texture Depth) data obtained using the laser profilometer, with the methods reviewed in this paper.

TEXTURE COARSENESS VS. PAVEMENT MACRO-TEXTURE

Of all textural features, coarseness is the most fundamental feature, such that in the narrowest sense, the term "texture" implied coarseness (Tamura 1978). Coarseness is a measure of the scale or element size, where images with larger element sizes are deemed coarser than those with smaller elements, or the larger the number of element repetitions per image region the finer is the region. Therefore in order to quantify coarseness, we require an algorithm that would consistently translate a region of a textured image into a coarseness number. Several algorithms have been developed and a few of them are explored in this paper. We first examine from existing literature whether texture coarseness is related to road surface macro-texture

To characterize road surfaces Schonfeld (Schonfeld1970) captured seven parameters from the surfaces using a stereoscopic device. One of the parameters was the "density of spacing" of the aggregates which is tantamount to saying "the number of elements (aggregates) in a given region". This corresponds well with the definition of coarseness of aggregates in 2D analysis of images.

Fourier analysis is used in texture analysis, and especially for the feature of coarseness in textures. The notion of characterising texture from its spectral characteristics in the frequency domain dates back at least to the work by Haralick *et al* (Haralick 1973). More recent implementations of Fourier techniques in texture analysis include the use of Gabor filters (Manjunath, et al 2001), which are scaled and shifted modulated Gaussians in the frequency domain. Incidentally (Gransberg 2002, Pidwerbesky 2006 and ElGendy 2008) also applied Fourier techniques to analyse road surfaces in the same manner that texture coarseness is handled in the Fourier domain. One such manner is the usage of frequency bands (or wavelength bands) to characterise road surface texture depth (Pidwerbesky 2006 and ElGendy 2008). These are a few examples that demonstrate that texture coarseness is related to surface texture depth.

However, texture coarseness analysis techniques are not solely restricted to Fourier domain analysis, and therefore texture depth from road surface images can also be analysed by other texture analysis techniques available in the literature. In this paper we explore two techniques in addition to the Fourier technique and discuss the results.

TEXTURE COARSENESS ANALYSIS TECHNIQUES

The equivalence of road surface macro-texture (depth) and the 2D surface coarseness is the single most important factor in using 2D image analysis techniques for macro-texture analysis. Therefore the question is one of finding the best algorithm that would consistently map 2D coarseness values into 3D texture depth. In this paper we explore three classical texture analysis methods including re-examining the frequency domain analysis using FFT. We then compare the performance of the selected methods with the SMTD (sensor measured texture depth) obtained from the laser profilometer. The data used was obtained from Nudgee Road (Fig.10). Fig.1 shows two samples from the road surface to demonstrate the fineness and coarseness levels encountered.

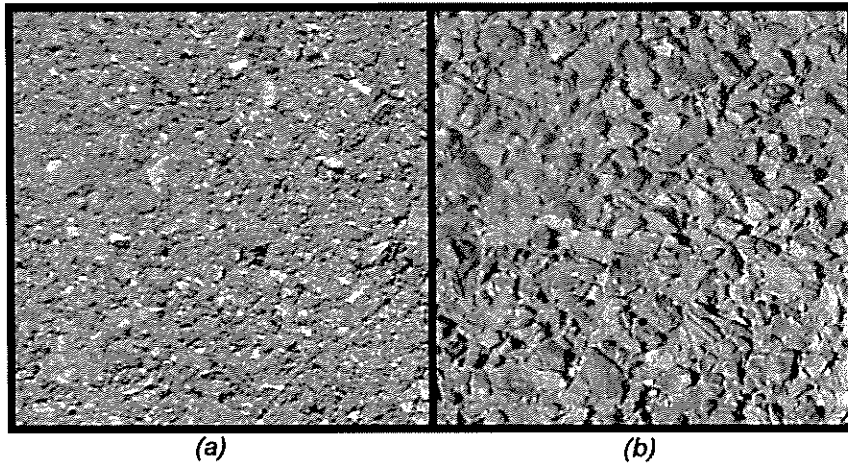


Figure 1: An example of a (a) fine and (b) coarse texture

Fourier Domain Analysis

The Discrete Fourier Transform $F(u, v)$ of an image $I(i, j)$ is defined as:

$$F(u, v) = \sum_{i=0}^{M-1} \sum_{j=0}^{N-1} I(i, j) e^{-j2\pi(ui/M + vj/N)} \quad (1)$$

Fig.2 shows the magnitude spectrum of the road surface images of Fig.1. Note that this is a centred Fourier transform, meaning the centre of the spectrum is the zero frequency component, and all regions in the proximity of this value are the low frequency components. The highest frequency (0.5 cycles/pixel), is a consequence of the Nyquist criterion which stipulates that a signal cannot have frequency components exceeding half the sampling frequency. The frequency values along the x-axis and y-axis of Fig.2 are multiples of the sampling frequency.

Brighter regions in the normalised FFT representation of Fig.2 imply greater magnitude. Clearly, the coarser the aggregates, the greater the magnitude they display in the lower frequency. In the field of texture analysis Fourier spectra are especially useful for estimating coarseness, but also effective in estimating directionality and regularity of textures. The orientation of the spectra could be used to extract directionality information, whereas periodicity in the spectrum could indicate a regular structure in the texture. (Manjunath 2001) compartmentalised the Fourier spectrum of images using Gabor filters, to obtain these features.

In the analysis of road surface macro-texture, neither directionality nor regularity are significant, and therefore the FFT spectrum is used purely for coarseness analysis, which contains information assumed to be proportional to texture depth. This is precisely the manner it was being utilised by (Pidwerbesky 2006).

A second popular method for texture coarseness analysis is the autocorrelation function.

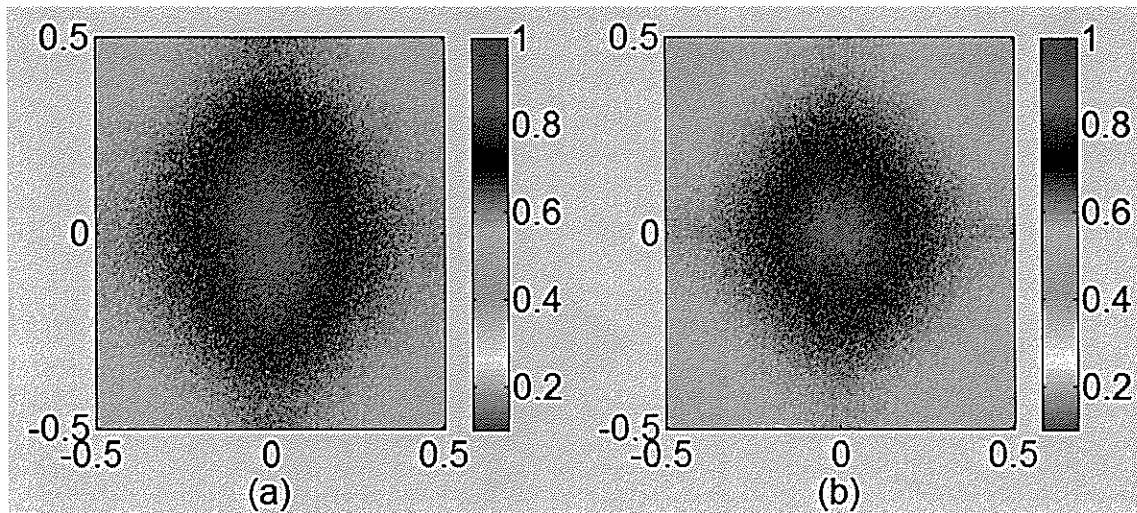


Figure 2: Frequency domain signature of the images in Fig.1. Notice the concentration of low frequency energy for the coarser image

Autocorrelation

The autocorrelation function $A[k, l]$ of an $M \times N$ image $I(i, j)$ is defined as follows:

$$A[k, l] = \frac{\frac{1}{(M-k)(N-l)} \sum_{i=1}^M \sum_{j=1}^N I[i, j] I[i+k, j+l]}{\frac{1}{MN} \sum_{i=1}^M \sum_{j=1}^N I^2[i, j]} \quad 0 \leq k \leq M-1, 0 \leq l \leq N-1 \quad (2)$$

Fig.3 shows a three dimensional display of the symmetric autocorrelation function $A[k, l]$ for the images in Fig.1, for lags of up to 50 pixels. The autocorrelation function drops off slowly when the texture is coarse, and rapidly for fine textures. The method has been used for estimating grain size in sediments by (Rubin 2004) with promising results. This can potentially be used to determine the relative coarseness of road surface texture. In order to examine the decay of the autocorrelation function with lag we use the representation of Fig.4, which clearly shows the slope for each of the autocorrelation functions in Fig.3 with the values squared, to remove negative values. For each curve in Fig.4 the slope (gradient) is calculated at each point. The slope is simply an indicator of how fast the vertical y-axis drops for every pixel change in the x-axis. Thus coarseness is inversely proportional to slope. Results showing how this method compares with the SMTD data are presented in Fig. 14, 15 and Table 1.

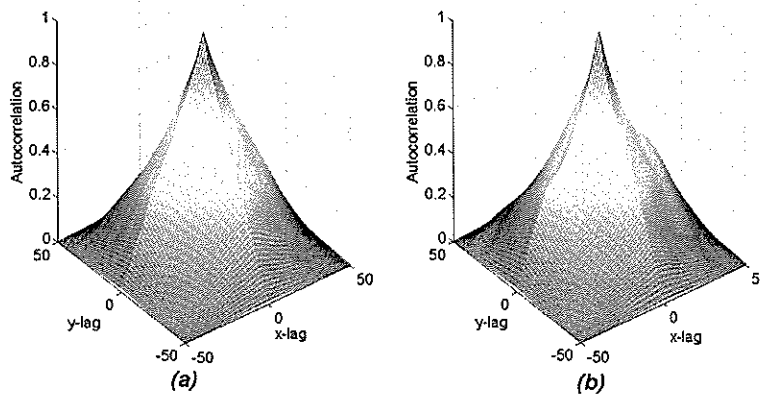


Figure 3: The autocorrelation of the images in Fig.1

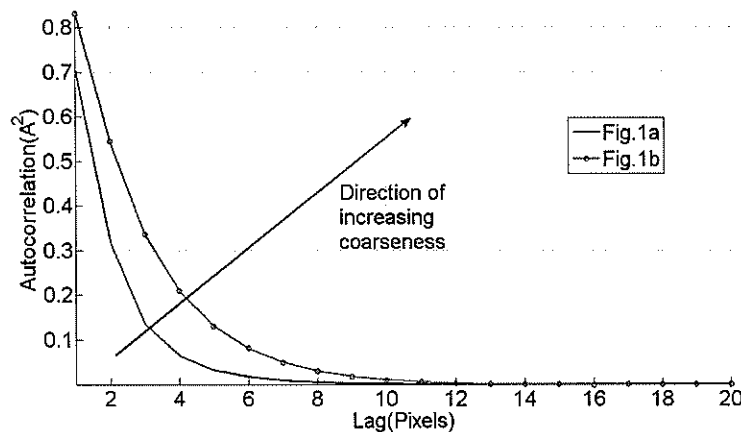


Figure 4: The autocorrelation sequences of the images in Fig.1. This is a comparison for the slopes of the cones in Fig.3

Wavelets

The representation of the road surface images in the Fourier domain, as in Fig.2 is based on $e^{-j2\pi(ui/M + vj/N)}$ basis functions. In effect the Fourier domain intensity images in Fig.2 depict points where the images in Fig.1 resonate with the two dimensional basis functions $e^{-j2\pi(ui/M + vj/N)}$. Representation of localised structure such as road surfaces, with infinite extent basis functions such as $e^{-j2\pi(ui/M + vj/N)}$ may incur an error. For this reason basis functions of finite extent have been developed and used to represent such localised signals with relative accuracy. This is the concept behind wavelet analysis of signals and images.

Wavelets are signals of limited duration that can be shifted and dilated, thus making them suitable for signal representation at various scales. A review of wavelets as used in signal and image processing can be found in (Gonzales 2008). Wavelet analysis of textures is a relatively young field of research, less than two decades old, commencing from the pioneering work of Unser (Unser 1992), but the volume of work pertaining to applications of wavelets to texture analysis to date has been significant.

We note that the manner in which we use the wavelet transform here is not similar to its traditional usage in texture analysis. The reason is that the outcome we seek in analysing road surfaces is slightly different from the traditional approach to texture analysis. Whereas in traditional texture analysis, wavelets were chiefly used for classification based on texture features, we use them here for computing a coarseness number, based on the image statistics of the wavelet-treated road surface images. To that end an understanding of three basic

concepts of wavelet analysis is required, namely, multiresolution, scaling functions, and wavelet functions.

Multiresolution analysis

Multiresolution analysis (MRA) refers to the analysis of signals at multiple resolutions. The idea is to represent a discrete signal $f(n)$ using a series of functions of decreasing resolution in such a way that it is possible to reconstruct $f(n)$ back from the functions. In Fig.5 the signal $f(n)$ is decomposed to its low pass and high pass components using special filters $L(n)$ and $H(n)$. These filters are necessarily related to each other in order to achieve certain properties of the resulting decomposition. One such property of the decomposing filters is that they make the reconstruction of the original signal $f(n)$ from the decomposed signals, possible. If reconstruction is not important, as it is in many texture analysis applications, then the relation between the decomposition filters could be relaxed.

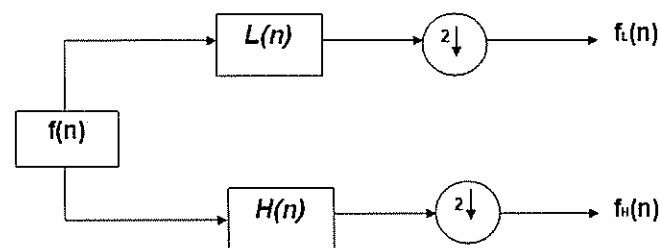


Figure 5: Decomposition of a signal to Low pass approximation and high pass details with sub sampling. Examples of low-pass and high-pass filters are shown in Fig.9

Two signals result from the decomposition of the signal $f(n)$ (Fig.5). The resulting low pass signal $f_L(n)$ can be further filtered and sub-sampled into low pass and high pass components, and this could be done indefinitely or till there is no signal left to decompose. Fig.9 shows the discrete low-pass and high-pass filter pairs, $L(n)$ and $H(n)$, for three types of wavelets. The relationship between $L(n)$ and $H(n)$ is determined by whether the filters are *orthogonal* or *bi-orthogonal*. Orthogonality and biorthogonality specify the relationships between the decomposition and reconstruction filters required for perfect reconstruction of a decomposed image. Reconstruction of the image is not important to our intended application, but these filters could still be used for the analysis stage to extract texture coarseness as was implemented in (Unser1992). DaubN is the class of Daubechies wavelet filters sharing the same properties. The length of each filter is given by $2N$. Similarly CoifN is the class of For Coiflets class of filters where the length of each filter is given by $6N$. Both DaubN and CoifN have the common property of orthogonality in their filters.

For orthogonal setting, one can infer the high-pass filter from the low-pass filter, and vice-versa. This is demonstrated in Fig.9 where the high-pass filter coefficients for Daub4 and Coif2 pairs (rows 1 and 3) are derived by reversing the order of the low-pass filter coefficients and then reversing the sign of every second one. Daub4 and Coif2 are orthogonal filters. For biorthogonal filters (bior3.5), they have to satisfy the biorthogonality condition, which effectively requires two filters (either the decomposition or reconstruction) to be specified. For the class of biorthogonal filters biorM.N, the length of the filter is $\max(2M, 2N)+2$. (Daubechies1992) and (Chui1992) provide excellent mathematical background on wavelet analysis and associated filters, and (Gonzales 2008) discusses wavelet implementation in image analysis. The wavelet toolbox in Matlab[®] provides in-depth information regarding the properties of wavelets filters.

Fig.6 shows the decomposition of an image into four sub-sampled components using low-pass and high-pass filters. The image is first filtered column-wise using both filters and then sub-sampled (also column-wise). The resulting images are again filtered using both filters row-wise with sub-sampling. These processes result in four decomposition images arranged as illustrated in Fig.7 and 8.

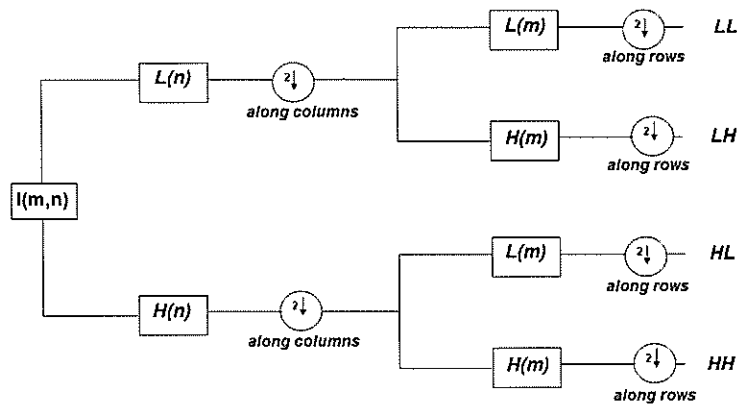


Figure 6: Wavelet decomposition of an image using Low-pass and High-pass filters.

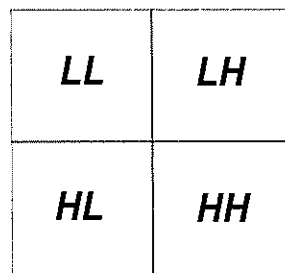


Figure 7: The resulting decomposition layout (see Fig.8)

Scaling functions and Wavelets

The filters L and H shown in the schema in Fig.5 and 6 are simply discrete versions of basis functions known as scaling functions and wavelets, respectively. Thus any signal could be represented by a scaling function and a set of wavelets. The closer the shape of the original signal is to the scaling function, the better the approximation. Therefore the choice of scaling functions and wavelets (also known as father wavelet and mother wavelet respectively) have an influence on the accuracy of the analysis of signals and images. In our case, since we are dealing with discrete images, the choice of the filters L and H influences the outcome of the results.

Although wavelets are suited for capturing textural properties, it is not yet clear which wavelet type is most suitable for capturing the coarseness of road surface macrotecture. Therefore we test three wavelets shown in Fig.9 below and empirically determine which class of wavelets are suitable for the class of data collected. This is done as follows: Each image is decomposed into its 4 components, and the energy (gray level variance) in the LL component (see Fig.8) is computed. The LL component is then further decomposed resulting in another LL in level2 and the variance also computed and so on. This is done for each image after which the effectiveness by which the energy in each decomposition level closely approximates texture depth, is established by correlating the energy results from each decomposition level with the SMTD values. Fig.8 is an example of a two level decomposition of a road surface image, using Coif2 filters (third row in Fig.9). The energy is obtained from the LL approximation images shown in the figure, whereas the detail images, three in each decomposition level, are discarded.

Performance results for the wavelet techniques are presented in the results section.

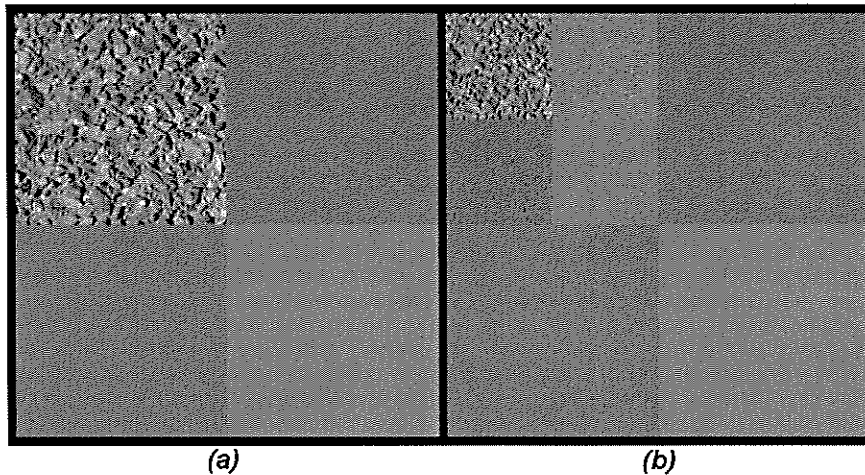


Figure 8: (a) Level 1 and (b) Level 2, wavelet transforms for the image in Fig.1b using Coiflet2

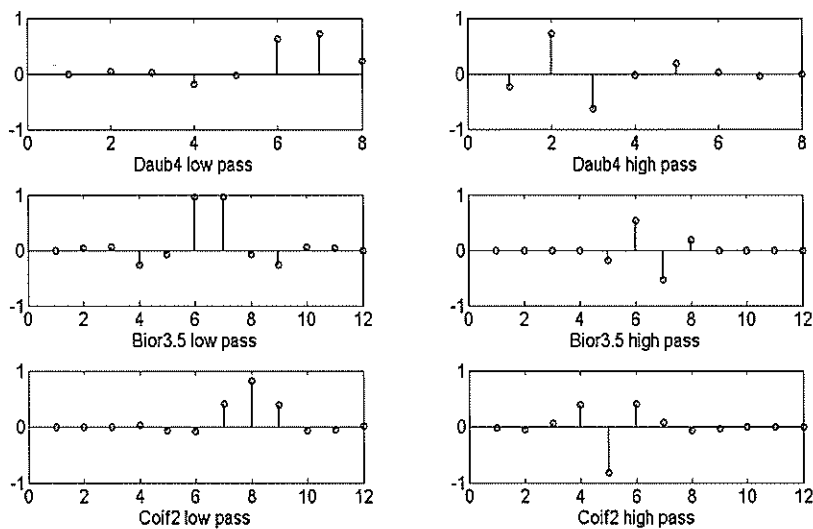


Figure 9: Three examples of low-pass (left column) and high-pass (right column) filters used in wavelet analysis. The three sets of filters are used in our experiments for comparison

DATA COLLECTION

Data sets were obtained from Nudgee road and portions of O'Quinn Street, at Nudgee Beach-Queensland, Australia shown in Fig.10, giving a combined length of more than 2km's. Images were acquired at approximately every 10m. SMTD data obtained from a laser profilometer were also collected about six months prior to the image acquisition. No maintenance was carried out during the six month period in between the acquisition of both data sets. Images were acquired from the BWP (between wheel path) portion of the road, to ensure a more valid comparison with the SMTD data. The still Images were acquired from a height of 80cm above road surface using a 7.2 Megapixel resolution camera.

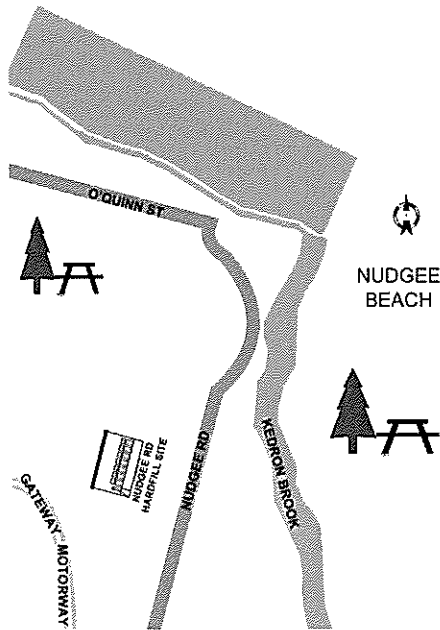


Figure 10: Section of road in Nudgee Beach where data was acquired

RESULTS

Results obtained from using the Fourier transform, the autocorrelation function and wavelets are presented here. For each technique, there are more than 110 data points for comparison with SMTD. By removing outliers, the correlation of any of the methods with SMTD improves. The results for all three methods are summarised in Table 1.

The purpose of using different wavelet filters was to investigate whether road surface macro-texture responds preferentially to a particular filter. There were no significant differences in the results from each of the three wavelet filters. The performance of each of the three chosen wavelet filters is shown in Table.1.

In correlating the results from the three methods (FFT, autocorrelation and wavelets) with the SMTD data, we note that the SMTD data is not in itself an absolute benchmark for road surface macro-texture, and therefore outliers may necessarily need to be removed. Rejecting outliers is generally a controversial practice; however, it is common where sources of measurement errors are easily identifiable. One source of error is the acquisition of data while in motion, which applies for both the laser and imaging methods. Despite the efforts in minimising motion induced errors, such errors cannot be completely removed. There will be some outliers, and the best way therefore is to gather a large number of data. However, the ideal case is to remove as few outliers as possible and still obtain good results.

Here we present results when outliers of up to 10% are removed. This roughly corresponds to a maximum of 12 points removed from the dataset. In general the wavelet method seems to perform better as more outliers are removed.

The results are displayed in Table.1 and Fig.11 to 17.

The FFT results displayed in Fig.11 highlight the superior performance at certain bands of the FFT method. This confirms that road surface macrotexture is sensitive to certain frequency of fluctuations. This observation was also made by in Pidwerbersky et.al (Pidwerbersky2006). To establish the results in Fig.11 we used the Fourier transforms of each image, such as that shown in Fig.2, and applied circular masks of increasing radii with fixed interval and centred at the origin. The resulting energy due to each mask was computed and the difference between the energy due to successive masks was considered as the energy of a band. This is equivalent to the energy due to a circular ring formed by the difference between two successive circular discs. In (Pidwerbersky2006), square masks rather than circular masks were used, resulting in rectangular rings, but arriving at similar conclusions regarding band sensitivity.

Table 1: Coefficient of determination (R^2) values, for the autocorrelation method (using image slope at lag=2), and wavelet methods for selected filters

% outliers removed	FFT method	Autocorrelation Method	Wavelet Method		
	Band-4	(1/slope) vs. SMTD	db4	bior3.5	coif2
0	0.700	0.638	0.676	0.652	0.677
1	0.744	0.697	0.769	0.736	0.771
2	0.756	0.735	0.792	0.761	0.792
3	0.755	0.767	0.803	0.791	0.804
4	0.767	0.782	0.805	0.805	0.820
5	0.773	0.787	0.821	0.821	0.821
6	0.780	0.800	0.831	0.840	0.832
7	0.786	0.799	0.838	0.847	0.839
8	0.797	0.804	0.850	0.858	0.851
9	0.801	0.817	0.856	0.862	0.856
10	0.808	0.823	0.858	0.866	0.858

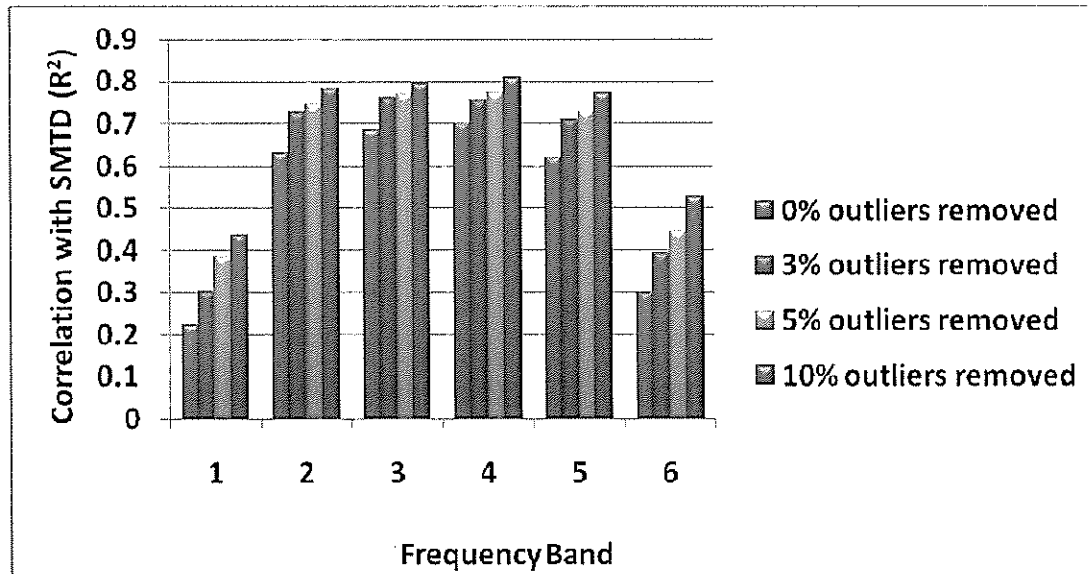


Figure 11: Coefficient of determination of Fourier frequency bands. Bands 3 & 4 show optimal performance.

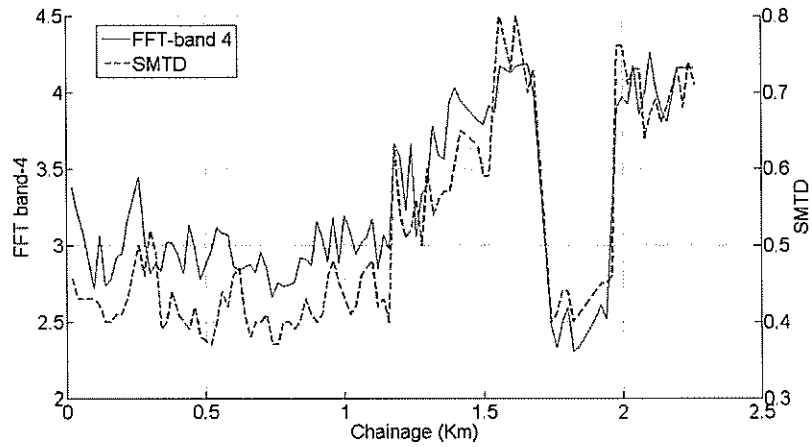


Figure 12: FFT (band 4) and SMTD, after removing 10% of outliers.

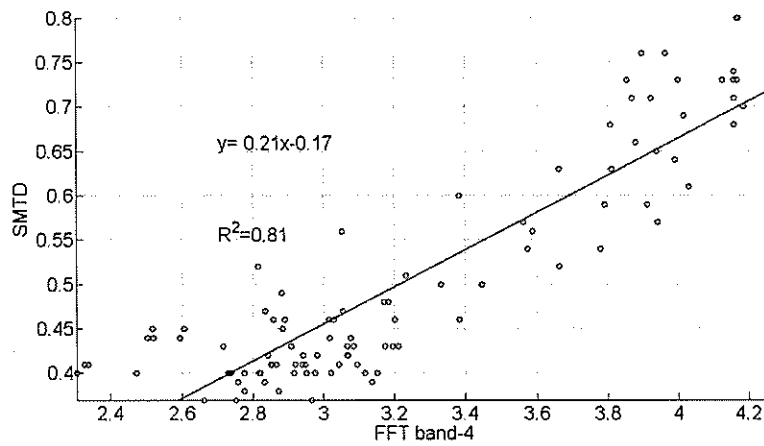


Figure 13: Correlation of FFT (band 4) and SMTD, after removing 10% of outliers.

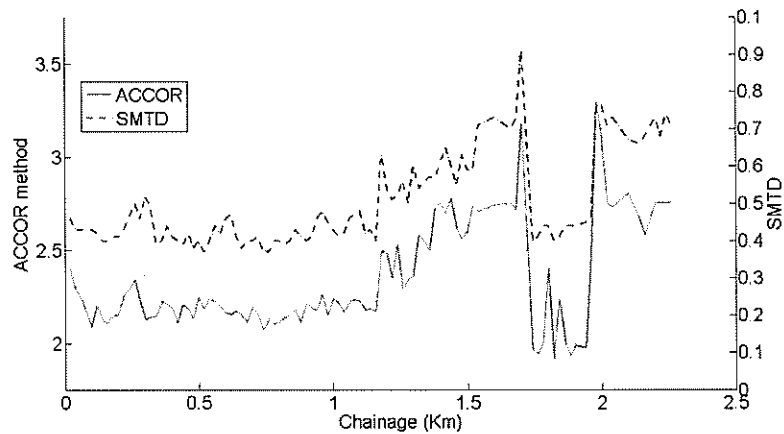


Figure 14: Autocorrelation method and SMTD, after removing 10% of outliers.

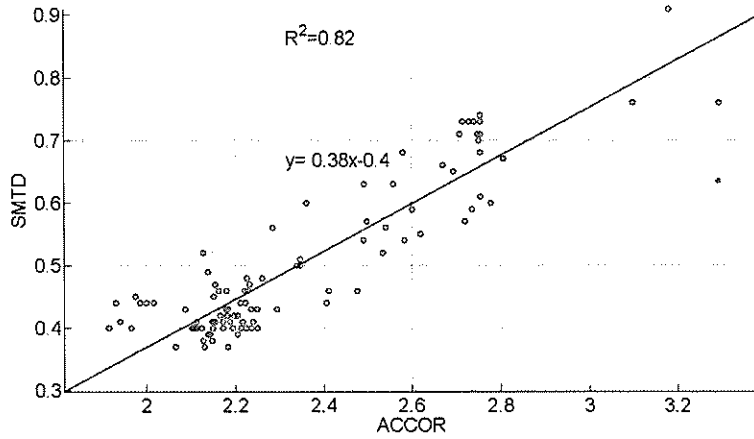


Figure 15: Correlation between the Autocorrelation method and SMTD, after removing 10% of outliers

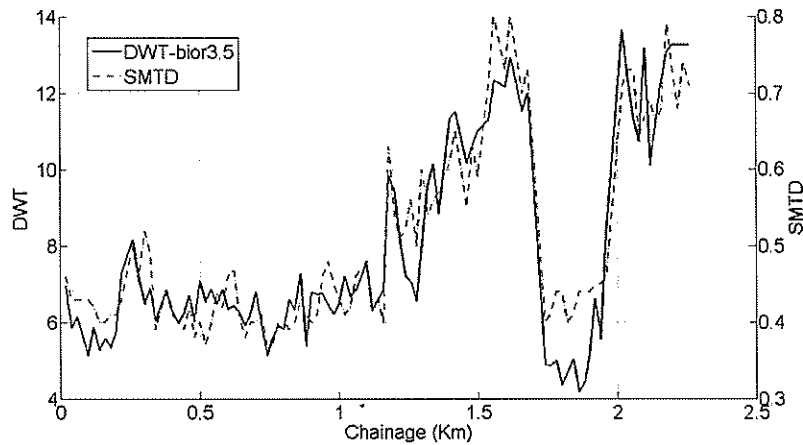


Figure 16: Wavelets (Bior3.5) method and SMTD, after removing 10% of outliers.

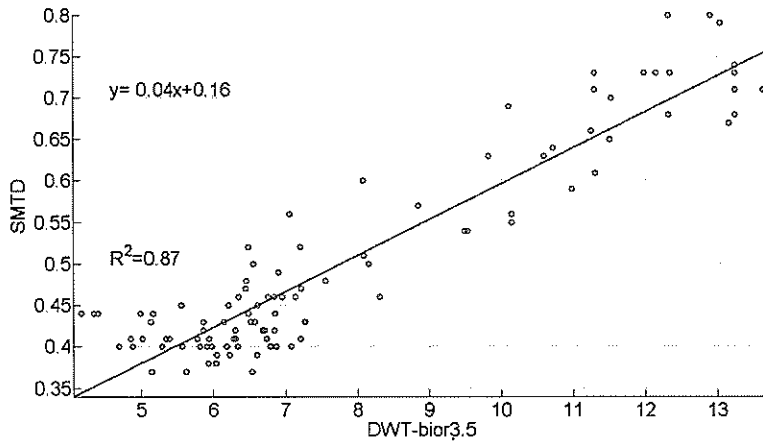


Figure 17: Correlation between the Wavelet (Bior3.5) method and SMTD, after removing 10% of outliers

DISCUSSIONS

The results indicate that spectral and statistical techniques for coarseness analysis are suited for texture depth analysis. We also confirm that there is a preference for certain FFT bands in the analysis of macro-texture in agreement with previous work (Pidwerbesky 2006, Elgendy 2008). The results from the wavelet analysis are also indicative of band selectivity as the best correlation with SMTD data is observed at the 4th level and in some cases the 3rd level decomposition. These are similar to the results obtained from the Fourier analysis results.

Fig.11 shows optimal performance for bands 3 and 4, but we believe this to be chiefly due to the image scale, as it can be shown that a zoomed-in image of aggregates appear coarse and therefore show preference to low frequency bands as opposed to the same surface obtained at a much smaller scale which would respond to high frequency bands. Thus, standardising the scale used in acquiring images would be a step closer to a harmonised method.

The resolution of the images acquired is at about 3 pixels/mm. According to (PIARC 1987) macro-texture ranges from 0.5mm to 50mm in wavelength. There seems to be a relationship between texture wavelength, texture depth, image resolution and the frequency band of the FFT/or the decomposition level of wavelets. The nature of this relationship is not clear at this stage and requires further research.

The results from the autocorrelation method also indicate that macro-texture responds to certain lags more than others. These optimal lags (in pixels) are related to what constitutes macro-texture. In Fig.3 we observe that a lag of 2 pixels is more likely to give a gradient value that would discriminate between various coarseness levels. This is a function of image resolution. High resolution images may show higher lag values that correlate better with SMTD.

The wavelet filters considered here are amongst the popular ones used in the image analysis literature, but they are a tiny subset of the available class of wavelets. For example bior3.5 is used in Jpeg2000 compression, and daub4, coif2 are applied in various studies of texture analysis. Judging by the results from these filters as displayed in Table.1 there is no indication of any particular preference, though bior3.5 filter slightly outperform the rest. Thus wavelet techniques in general are well suited for the task of road surface macrotecture analysis.

The FFT and autocorrelation techniques are not far behind either in comparison with wavelets, and it might be the case, that the available data favoured wavelet techniques at this stage. Extensive experimentation requires to be done in order to arrive at a conclusive performance merit regarding the different techniques. It suffices, for now, to say that imaging techniques hold a promise in the field of macrotecture analysis of road surfaces.

The outliers removed, in correlating the results from the different methods with SMTD, are different in each case. It is observed that the 10% outliers removed when using the FFT method and the wavelet method, result in SMTD values ranging roughly from 0.3 to 0.8. The 10% outliers removed when using the autocorrelation method, result in SMTD values ranging roughly from 0.4 to 0.9. For this reason the SMTD scales are not uniform in all cases. A Uniform SMTD scale is possible if the comparisons are made with no removal of outliers.

Some of the challenges associated with imaging techniques that require to be addressed include, characterizing the effects of illumination, effects of surface gray level resulting from different surface types, effects of resolution and whether images could be acquired at highway speeds similar to the laser profilometer's 90km/h. The efficacy of digital image processing approaches depends on addressing these challenges.

For consistent results across road surfaces it is recommended that the level of lighting be fixed at a known level. The precise effect of lighting on the coarseness of the image is currently being studied. The images for the experiments in this paper were acquired on a sunny morning between 10am and 12pm. The method is also limited at this stage to asphalt concrete surfaces and tests on other surfaces are required for further validation. The effect of image resolution has been discussed in the context of Fig.11 and therefore a standardized image resolution is essential for a consistent result. Another issue associated with the imaging method is storage and image capture rate especially at the maximum speeds by which the laser profilometer operates that is, 90km/h. The images in our experiments were captured at roughly 10m

intervals, and therefore at 90km/h (25m/s), this implies a steady capture of 2.5 (roughly 3) still images per second. This means that in order to scan a road extending 20km at a steady speed of 90km/h, 2400 images is captured. At 2M/image, this amounts to 4800M or 4.8G of data. In our experiments we used 1M portion of the entire 6M of images captured.

Consequently, there is an obvious disadvantage of imaging techniques with respect to data storage in comparison to laser scanning methods. However, this size of data with today's storage capacities ceases to be a problem but rather some advantages could be pointed out. For one, imaging techniques will allow for manual verification by an expert. Secondly, an operator can choose to precisely locate a patch of road visually prior to acquisition of data.

CONCLUSION

We have presented some further evidence that digital image processing techniques for texture analysis could be applied to texture depth analysis and used for analysing macro-texture on road surfaces. It is also apparent that the results are influenced by the acquired image resolution, acquisition height, and possibly illumination levels and therefore further research is required to quantify these effects.

REFERENCES

ASTM E2157-01, Standard test method for measuring pavement macro-texture properties using the circular track meter, ASTM STD 2005

Butler, J, Lane, S and Chandler, J , *Automated extraction of grain-size data from gravel surfaces using digital image processing*, Journal of Hydraulic research, vol. 39 No 4, 2001.

Choi, Y, *Review of surface texture measurement method for seal design input*, Austroads, Tech. Rep., 2008.

Chui, C.K, *An Introduction to Wavelets – Wavelet Analysis and Its applications*, series – Academic Press, 1992

Daubechies, I, *Ten Lectures on Wavelets*, Society for Industrial and Applied Mathematics (SIAM), 1992

El Gendy, A and Shalaby, A, *Image requirements for three-dimensional measurement of pavement macro-texture*, Journal of the Transportation Research Board, vol. 2068, pp. 126–134, 2008.

Gransberg, D., Karaca, I., and Burketi, W, *Quantifying Seal Coat Surface Condition Using Digital Image Processing Based on Information Theory*, The International Journal of Pavement Engineering, 2002 Vol. 3 (4), pp. 197-205.

Gonzales, R and Woods, R.E, *Digital Image Processing*, 2nd Ed. New Jersey: Prentice Hall, 2008.

Haralick R.M, Shanmugam, K and Dinstein, I, *Textural Features for Image Classification*, IEEE Transactions on Systems Man and Cybernetics, vol. SMC-3, no. 6, Nov. 1973, pp 610-621

Laws, K, *Textured image segmentation*, Ph.D. dissertation, University of Southern California, Jan. 1980.

Manjunath, B.S, Ohm, J.R, Vasudevan, V.V and Yamada, A, *Color and texture descriptors*, IEEE Transactions on Circuits and Systems for Video Technology, vol. 11, no. 6, 2001, 703 - 715.

PIARC, *Technical Committee report on Surface Characteristics*, XVIIth World Road Congress, Brussels, 13-19 Sept. 1987

Pidwerbesky, B, Waters, J , Gransberg, D and Stemprok, R, *Road surface texture measurement using digital image processing and information theory*, Land Transport New Zealand, Tech. Rep., 2006. [Online]. Available: <http://www.landtransport.govt.nz/research/reports/290.pdf>

Rubin, D, *A simple autocorrelation algorithm for determining grain size from digital images of sediment*, in *Journal of Sedimentary Research*, pp 160-165, vol. 74, No.1, 1 January 2004.

Schonfeld, R. *Photo-Interpretation of Skid Resistance*, Highway Research Record: No. 311, 1970.

Tamura, H, Mori, S and Yamawaki, T, *Textural features corresponding to visual perception*, IEEE Transactions on Systems Man and Cybernetics, vol. smc-8, No.6, 1978.

Unser, M, *Texture Classification and Segmentation Using Wavelet Frames*, IEEE Transactions on Image Processing, Vol.4, No.11 Nov 1995

ACKNOWLEDGEMENT

The authors would like to acknowledge Mr. Hari Krishnan, of the Pavement Performance and Investigation section of the Queensland Department of Transport and Main roads, for his provision of the SMTD data used in this research.

AUTHOR BIOGRAPHIES

Ronald Elunai obtained his B.Eng Electrical and Computer (Hons.1) from Queensland University of Technology in 2004. His current position is Engineer at ITS and Electrical Technology in the Department of Transport and Main Roads (DTMR) – Queensland. Ronald is currently completing his PhD thesis in Particulate texture analysis and its applications.

Vinod Chandran is a professor in the School of Engineering Systems at the Queensland University of Technology, Brisbane, Australia. He earned a PhD in Electrical and Computer Engineering from Washington State University, USA, in 1990. His research interests span signal and image processing and their applications. He has supervised 9 PhD and 2 Masters by research to completion in these areas.

Prosper Mabukwa joined DTMR in October 2006 as a Senior Electrical Engineer. Currently he is Principal Engineer (ITS Projects) at the Metropolitan region Brisbane. Prosper graduated with a BSc Electrical Engineering Honours Degree from the University Of Zimbabwe in 1987 and obtained a Master of Business Administration Degree from the same University in 1998. He is a member of Engineers Australia and takes a keen interest in the application of mathematical and engineering techniques in solving challenges facing business today.

Copyright Licence Agreement

The Author allows ARRB Group Ltd to publish the work/s submitted for the 24th ARRB Conference, granting ARRB the non-exclusive right to:

- publish the work in printed format
- publish the work in electronic format
- publish the work online.

The author retains the right to use their work, illustrations (line art, photographs, figures, plates) and research data in their own future works

The Author warrants that they are entitled to deal with the Intellectual Property Rights in the works submitted, including clearing all third party intellectual property rights and obtaining formal permission from their respective institutions or employers before submission, where necessary.